Mansoura Engineering Journal

Volume 34 | Issue 4 Article 15

12-1-2020

Natural Convection Heat Transfer from a Heat Sink with Hollow/ Perforated Circular Pin Fins.

E. Elshafei
Department of Mechanical Power Engineering, Mansoura University, Mansoura, EGYPT,
eeshafel@mans.edu.eg

Natural Convection Heat Transfer from a Heat Sink with Hollow/ perforated circular Pin Fins

إنتقال الحرارة بالحمل الحر من بالوعة حرارية ذات زعانف مفرغة دائرية المقطع ومثقوبة

*E. A. M. Elshafei

Department of Mechanical Power Engineering, Mansoura University, EGYPT
*Corresponding author, Fax: +202 50-2244690
E-mail: eelshafei@mans.edu.eg

ملخص البحث:

أجريت تجارب على إنتقال الحرارة بالحمل الحر من بالوعات حرارية ذات بنوز دائرية المقطع مصمتة ومفرغة من الداخل / ومثقوبة بثقب واحد على مسافة 5 مم من القاعدة لبيان تأثير الفيض الحرارى وزاوية الميل ونسبة القطر الداخلى الى القطر الخارجى للبنز على أدائها. تم تثبيت البنوز على القاعدة ووزعت بطريقة تبادلية. البنوز والقاعدة مصنوعة من الألومنيوم. تمت التجارب فى حجرة بالمعمل بعيدة عن أية تيارات هوائية لوضعين مختلفين للبالوعة: الأول البنوز مواجهة لأعلى (القاعدة أفقية) والثانى البنوز أفقية (القاعدة راسية) لمدى تغير رقم رايلى $4.5\times10^{6} \le Ra \le 1.65\times10^{7}$. تبين من النتائج أن معامل انتقال الحرارة للبالوعة ذات البنوز المصمتة فى وضعيها المواجه لأعلى والأفقى متقارب ويتبادلان فى قيمهما من حيث الزيادة والنقصان تبعا لقيمة معامل رايلى ، وفى المجمل أعلى منه لذات البنوز المفرغة. على الجانب الأخر فإن البالوعة ذات البنوز المفرغة أدائها أفضل عندما تكون البنور أفقية عنة عندما تكون راسية ، وأن نسبة الزيادة لمعامل انتقل الحرارة ترتفع بزيادة نسبة القطر الداخلى الى القطر الخارجى للبنز (Di/Do). وأظهرت النتائج أيضا أن الأداء الحرارى للبالوعة ذات البنوز المفرغة فى الوضعين أفضل من ذات البنوز المصمتة من حيث الفرق بين درجتى حرارة سطح البالوعة المتوسط والهواء المحيط وأن هذا التحسن فى الأداء يزداد بزيادة Di/Do.

Abstract

Experiments were performed on natural convection heat transfer from circular pin fin heat sinks subject to the influence of its geometry, heat flux and orientation. The geometric dependence of heat dissipation from heat sinks of widely spaced solid and hollow/perforated circular pin fins with staggered combination, fitted into a heated base of fixed area is discussed. Over the tested range of Rayleigh number, $4.5\times10^{6}\le Ra\le1.65\times10^{7}$, it was found that the solid pin fin heat sink performance for upward and sideward orientations shows a competitive nature, depending on Rayleigh number and generally shows a higher heat transfer coefficients than those of the perforated/ hollow pin fin ones in both arrangement. For all tested hollow/perforated pin fin heat sinks, however, the performance for sideward facing orientation was better than that for upward facing orientation. This argument is supported by observing that the augmentation factor was around 1.05-1.11, depending on the hollow pin diameter ratio, Di/D_o. Meanwhile, the heat sink of larger hollow pin diameter ratio, Di/D_o, offered higher heat transfer coefficient than that of smaller Di/D_o for upward orientation, and the situation was reversed for sideward orientation. The heat transfer performance for heat sinks with hollow/perforated pin fins was better than that of solid pins. The temperature difference between the base plate and surrounding air of these heat sinks was less than that of solid pin one and improved with increasing Di/D_o.

Keywords: Energy efficient; Natural convection; Round/ hollow pin fins; Heat sinks; Orientation effects; Electronic cooling.

1. Introduction

For many industrial applications, heat generation can cause overheating problems and sometimes leads to system failure. To overcome this problem, efficient heat sinks are essential. Natural convection from these devices is one of the considered cooling techniques and played an important role in maintaining their reliable operation. In such circumstances, the heat sink may consume up to 40% of the total system volume. Therefore, smaller and more compact one is needed. Due to their potentially high heat transfer characteristics, less sensitive to air flow pattern and surface area density [1, 2], round pin fin array heat sinks have been of interest to designers of electronic equipment and turbine cooling applications.

Accepted December 31, 2009.

Pin fins having a height, H_f to pin diameter, D ratio of $0.5<H_f/D<4$ are accepted as short fins, whereas long pin have $H_f/D > 4$ [3]. For short pin-fins, the pin's height–to-diameter ratio is the dominant factor influencing the heat transfer coefficients as reported by Tanda [3]. However, for $H_f/D > 3$, the array's rate of heat dissipation was increased with the increasing of H_f/D as concluded by Armstrong and Winstanely [4].

Nomenclature

A	surface area, m^2
D	pin fin diameter, mm
g	gravity, m/s^2
H_f	pin fin height, mm
h	convective heat transfer coefficient, $W/m^2 K$
$\bar{h}$	average heat transfer coefficient, W/m^2K
k	thermal conductivity, W/m K
L	base plate length, m
N	number of pin fins
$\overline{Nu}$	average Nusselt number, dimensionless
Q	heat rate, W
Ra	Rayleigh number, dimensionless
S	pin spacing, mm
T	temperature, C
V	volume, m^3
W	base plate width
x	horizontal
y	vertical

Greek Symbols

α	thermal diffusivity of air, m^2/s
β	coefficient of thermal expansion of air, K^{-1}
ε	radiative emissivity, dimensionless
η_f	fin efficiency, dimensionless
η_o	overall efficiency, dimensionless
υ	kinematic viscosity, m^2/s
σ	Stefan-Boltzman constant, $W/m^2 K^{-4}$
ϕ	heat sink porosity dimensionless
Ψ	finning factor, dimensionless

Subscripts

a	air
bp	base plate
c	convection
con	conduction
f	fin
fp	projected fin
fm	mean fin
h	horizontal
i	inside, film
in	input
L	loss
Net	net
o	outside
rad	radiation
s	heat sink
sm	mean surface
surw	surrounding walls
t	total
v	vertical

Superscript

—	average quantity

While considerable information exists on convective heat sinks and plate fin arrays [5, 6], however, the available literature related to natural convection heat transfer from round pin fin arrays is relatively limited, especially those of perforated hollow pin fins. Early experimental study [7, 8] was presented for a set of five staggered, widely spaced cylindrical pin fins on plate that exchange heat by both natural convection and radiation. Their results revealed that the upward facing (horizontal base/vertical fin) orientation yielded the highest heat transfer rates, followed by the side-ward facing and the downward facing orientation ones. The radiation was found to be an important factor, contributing 25-45% of the overall heat transfer. Natural convection and radiation from an air-cooled, highly populated pin-fin array was investigated experimentally by Alessio and Kaminski [9]. The base plate was maintained in a vertical position while varying the pin inclination. It was reported that the arrays of 30° from the horizontal exhibited about a 10 % lower heat transfer rate than their horizontal counterparts and the performance of the 60° arrays was still worse (20-40 % lower than that of the horizontal array). Zografos and Sunderland [10] investigated natural convective heat transfer from inline and

staggered pin fin arrays. It is reported that the inline arrays gave higher heat transfer dissipation than the staggered ones, and the effect of orientation less than 30° from the vertical on arrays performance was relatively small. Aihara *et al.* [11] investigated experimentally a set of round pin arrays with a population density of 2.42 - 9.9 pins/cm^2. An empirical correlation for predicting the heat transfer performance of round pin fin arrays was established.

An experimental study was conducted on natural convection heat transfer from square pin fin and plate fin heat sinks subject to the influence of orientation by Huang *et al.* [12]. Over a tested range of $1.8\times10^6 < Ra < 4.8\times10^6$, it is reported that the downward facing orientation yielded the lowest heat transfer coefficient for both pin fin and plate fin geometry. It is also observed that the sideward arrangement outperforms the upward one for small finning factor, Ψ (which represents the total surface area, A_t divided by the base plate area, A_{bp}) and the situation is reversed for large finning factor as reported. In addition, the advantage of the pin fins escalates with the increase of the Rayleigh number due to the more open ends for air ventilation as reported. Enchao and Yogendra [13] investigated the enhancement of heat transfer from enclosed discrete heat source using pin fin heat sinks taking into account the three modes of heat transfer. Large deviations between the existed natural convection correlations for pin fin arrays in free space and their measured data were observed. They reported also that the enhancement of heat transfer rate was significantly affected by enclosure orientations. Vertical orientation of the enclosure produced lower thermal resistance.

Natural convection heat transfer from pin fin array with horizontal base was investigated by D. Sahray *et al.* [14]. It is reported that heat transfer enhancement due to the fins increased up to a certain fin number, and then decreased, demonstrating that an optimum array existed. A relative contribution of outer and inner fin rows in the heat sink was also assessed. Taking into account the edge effects, the role of the outer rows was dominant. This indicated that the heat sink could be built without inner fins at all. However, when the edge effects are supposed to be absent, the contributions of different fins became comparable as reported. An optimization of natural convection pin fin heat sinks fabricated of thermally conductive polyphenylene sulphide (PPS) polymer using Aihara *et al.* correlation [10] was carried out by Bahadur and Cohen [15]. It is reported that the rate of heat dissipation was greatly dependent on the geometrical parameters of the heat sink and the performance of such lighter fin array was about three times greater than that of the conventional aluminum one. Peterson and Ortega [16] have reviewed the use of natural convection, among other approaches, to cooling electronic equipment.

Analytical solutions for free convection limits for pin fin cooling were presented by Fisher and Torrance [17]. They suggested that the pin fin heat sink design could be optimized by proper choosing of both fin diameter and porosity, and the chimney effect was shown to enhance heat transfer. Kobus and Oshio [18] carried out an experimental and theoretical study on pin fin heat sink performance. A theoretical model was suggested to predict the effect of geometrical, thermal and flow parameters on the effective thermal resistance of heat sink. Subsequently, Kobus and Oshio [19] investigated the effect of thermal radiation on the heat transfer of pin fin heat sinks and presented an overall heat transfer coefficient related to both radiation and convective heat transfer modes.

The above literature indicates that many studies have been carried out for different types of fin arrays, but still there is lack of knowledge of the natural convection heat transfer from a surface with hollow perforated pin fins. The present work deals with the heat transfer performance of solid and

hollow/perforated pin fin heat sinks relying on natural convection. Parameters such as pin fin structure, and Rayleigh number, fit most specifications. In natural convection, the orientation of the heat sink plays an important role in its performance. The effect of pin diameter ratio (Di/Do) variation on the heat sink performance is investigated for horizontal/vertical base plate orientations. Furthermore, the heat transfer experiments of solid pin fin array are also conducted for the sake of performance comparison.

2. Experimental setup and procedure

2.1 Pin-fin assembly

A perspective view of the hollow/perforated heat sink is shown in Fig. 1a. It consists of an array of 8 round solid or hollow with single perforated pin fins (a) (Do =12 mm, H_f = 50 mm) screwed into the upper surface of the base plate (b) of a fixed area (150 mm x 150mm) and of 10 mm thickness as shown in Fig. 1b. The base plate and the pin-fins were made of aluminum with a thermal conductivity of 237 W/m K, and good contact between them was assured. The pin fins were widely spaced (S_h/D_o= 3.5, S_v/D_o= 5) and arranged in a staggered manner. All pin-fins were single perforated by a 3.5 mm drill bit, at 5 mm from the heat-sink base. These pins can be easily removed and drilled with pits of different diameter to have variable inside-outside diameter ratio (Di/D_o= 0, 0.33, 0.5, 0.66). The construction method was to screw the round aluminum pins into the predrilled base plate and the pin-fin's height was assured to be fixed in each test. Detailed dimensions of the test samples are listed in Table 1. and illustrated in Fig. 1

2.2 Heating System

During experiments, the heat sink base plate was heated by an attached electric heater (c) with an identical size as the base plate, which could supply a specific heat flux. The presence of thin layer of high thermal conductivity mica ensured that good thermal contact existed between the heater and the heat sink base. The side surfaces of the base plate as well as the heater block were insulated thermally with 50 mm gypsum (d) (k = 0.17 W/m K) and its lower side was insulated by 60 mm thick glass wool blankets (k = 0.04 W/m K). The whole assembly, base, heater with associated thermal insulation, was located in a well-fitting open-topped wooden box (f) of 25 mm thick as shown in Fig.1b. The upper edges of the wooden box and the top surface of the laterally-placed thermal insulation were flush with the upper surface of the heat sink base in which the pin fins protruded perpendicularly. The power supplied to the heater was controlled by a variac transformer to obtain constant heat flux along the base plate, and was measured by inline multi-meter (an ammeter and voltmeter).

A total of eleven copper-constantan (T-type) thermocouples were appropriately distributed among the base plate (Fig. 1c) to measure its average temperature, t_{bp}. These thermocouples were pressed into fine holes and glued in position with epoxy so as to ensure good thermal contact. To verify the quality of measurements, four T- type thermo-couples were glued into one of the pin fins; at the base, 1/3, 2/3 3/3 of its height to detect the mean fin temperature. Four T-type thermocouples were installed inside the insulation box at two cross positions to calculate the rate of heat loss from the bottom of the heater, Q_{cond}. All thermocouples were pre-calibrated with an accuracy of ± 0.1°C. The signals from thermocouples were transmitted to a multi-channel temperature recorder via a multipoint switch where temperatures can be measured and recorded. The whole assembly was located in an enclosed space inside the laboratory, far from any air disturbance promoters. Heat sinks of horizontal base plate (upward facing orientation) and of vertical base plate (sideward facing orientation) as shown in Fig. 2 were

tested in the enclosed room at nearly fixed temperature of 20°C with the power inputs ranging from 5W to 60 W. Steady state conditions was indicated by noticing the repeatable readings of each thermocouple at different locations of the heat sink. Each test run took nearly 2-hours to reach equilibrium when the power is turned on.

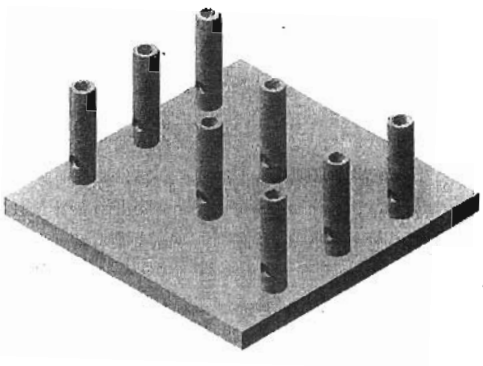

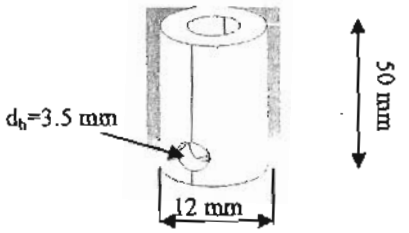

(a) Perspective view of Hollow/single perforated pin fin heat sink

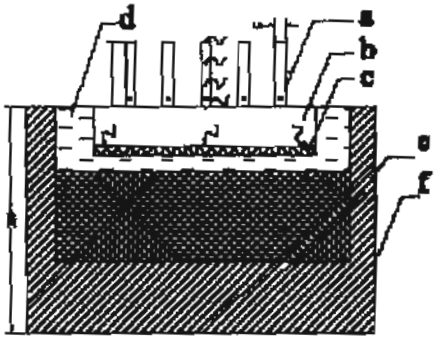

(b) sectional view of heat sink assembly

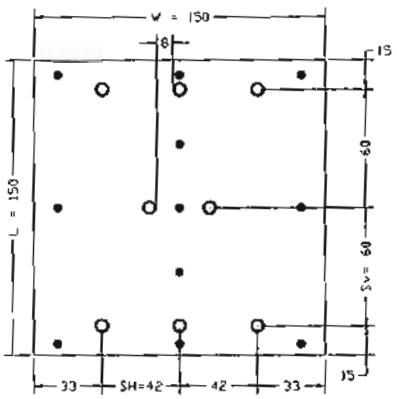

(c) thermocouple locations

Dimensions in mm

(a) Pin fins, (b) Base plate, (c) Heater, (d) Gypsum, (e) Glass wool insulation, (f) Wooden box

Fig.1 Details of pin fin heat sink assembly, heating unit and thermocouple distribution

Table 1: Geometric details of tested heat sink modules

	S_b (mm)	S_v (mm)	W, L (mm)	H_f (mm)	D_o (mm)	D_i (mm)	Ψ (A_f/A_{bp})
Sample1	42	60	150	50	12	0.0	1.71
Sample 2	42	60	150	50	12	4.0	1.94
Sample 3	42	60	150	50	12	6.0	2.05
Sample 4	42	60	150	50	12	8.0	2.15

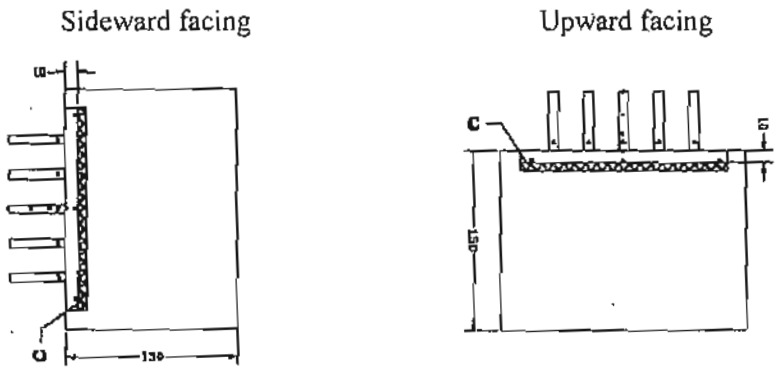

Fig. 2 Heat sink orientations

3. Data reduction

For the problem of interest, Q_{net} is transferred from a heated surface to its surrounding by both convection and radiation, given by

$$Q_{net} = Q_c + Q_{rad} \quad (1)$$

This net rate of heat exchanged can be described as

$$Q_{net} = Q_{in} - Q_{loss} \quad (2)$$

Where Q_{in} is the total power input to the heat sink is and Q_{loss} is the rate of heat loss by conduction from the backside and edges of the base plate surrounding ambiance.

Under the entire test conditions employed, the rate of heat loss by conduction ($Q_{loss} = Q_{cond}$) could be ignored. The pradiation contribution, Q_{rad} can be estimated following the procedure reported by Zografos and Derland [9] as

$$Q_{rad} = \frac{\sigma A_t \left(T^4_{sm} - T^4_{surw}\right) \varepsilon_s}{\left(1-\varepsilon_s\right) + \frac{A_t}{A_{surw}}} \quad (3)$$

Where A_t is the total surface area of the heat sink (the sum of fins area and that of the base plate), that is very small compared to the area of the surroundings walls, justifying the elimination of the last term (A_t/A_{surw}) in the above equation, σ is the Stefan-Boltzman coefficient, ε_s is the emissivity of the heat sink surface (oxidized aluminum, $\varepsilon_s \approx 0.15$) and T_{sm} is the average temperature of this heat sink. By subtracting the radiation contribution, Q_{rad}

from the net rate of heat exchanged, Q_{net} described in Eq. (1), the steady state rate of heat transferred from the heat sink by natural convection, Q_c can be determined. This rate of heat transfer by convection can be described as:

$$Q_c = \left(h_{bp} A_{bp} + h_f A_f \eta_f\right)\left(T_{bp} - T_a\right) \quad (4)$$

Introducing the overall fin efficiency, η_o term into the above equation, and considering that, $h_{bp} = h_f = \bar{h}$, then

$$Q_c = \bar{h} A_t \eta_o \left(T_{bp} - T_a\right) \quad (5)$$

The term η_o can be detected from the measured data $\left(\eta_o = 1 - \frac{A_f}{A_t}\left(1 - \eta_f\right)\right)$, η_f is the fin efficiency ($\eta_f = {T_{fm} - T_a}/{T_{bp} - T_a}$), and A_{bp}, A_f and A_t are the un-finned portion of base plate, pin fins and total heat sink surface areas (with the fin tip contribution assumed to be negligible) available for heat transfer, respectively, given by

$$A_{bp} = WL - A_{fp} \quad (6)$$

$$A_{fp} = N_f \frac{\pi}{4}\left(D_o^2 - D_i^2\right) \quad (7)$$

$$A_f = N_f \pi\left[\frac{1}{4}\left(D_o^2 - D_i^2\right) + \left(D_o + D_i\right)H_f + \left(D_o - D_i\right)d_h\right] \quad (8),$$

$$A_t = A_{bp} + A_f \quad (9)$$

Where L and W are the length and width of the base plate, respectively, D_o and D_i are the outer and inner diameter of the pin fin, respectively, A_{fp} is the projected area of pin fins, H_f is the pin fin height, d_h is the perforation diameter, and N_f is the total number of pin fins in the heat sink. (For solid pin fin, D_i =0.0 and d_i = 0.0).

The average convective heat transfer coefficient based on the total heat transfer surface area can be determined from Eq. (5) as

$$\bar{h} = {Q_c}/{A_t \eta_o \left(T_{bp} - T_a\right)} \quad (10)$$

The average Nusselt number, $\overline{Nu}$ definition based on the base plate edge, is given by

$$\overline{Nu} = {\bar{h} L}/{k} \quad (11)$$

The Rayleigh number, Ra is proportional to the temperature difference $(T_{bp} - T_a)$, which is the major driving potential throughout the experiments, and its definition based on the base plate edge can be expressed as:

$$Ra = {g\beta\left(T_{sm} - T_a\right)L^3}/{\upsilon\alpha} \quad (12)$$

The thermo-physical properties of the air appeared in the $\overline{Nu}$ and Ra numbers are evaluated at the film temperature, T_f, defined as

$$T_f = {\left(T_a + T_{sm}\right)}/{2} \quad (13)$$

The mean surface temperature, T_{sm} can be expressed as

$$T_{sm} = {\left(A_{bp} T_{bp} + A_f T_{fm}\right)}/{A_t} \quad (14)$$

- Measurement uncertainties

The experimental uncertainty is estimated using the uncertainty propagation equation proposed by Kline and McClintock [20]. As described in Eq. (10), $\bar{h} = f\left(Q_c, A_{bp}, \eta_f, T_a, T_{bp}\right)$, the measured uncertainties summed into the heat transfer coefficient are from the ambient and surface temperatures, the heat transfer surface area, and the total heat supply. In the present study, precautions were taken in establishing the

experimental rig to assure accurate measurements of temperatures and the power supplied to the base plate of the heat sink. Each of the stated dimensions was accurate to ± o.2 mm, and the measured temperature to ±0.2°C. The multi-meter has an accuracy of ± 1% reading + 4 dgt for the Ac Volts and ± 2% rdg + 4 dgt for the AC current. By substituting the measured data into the equation, the highest uncertainty for the heat transfer coefficient is about 11%, occurring at the lowest input power (5 W). This uncertainty decreases less than 4% when power input is larger than 10 W.

4. Results and discussion

4.1 Solid pin fin heat sink

For the sake of comparison, the solid pin fin array with the same dimensions of both the base plate and pin fins was first tested and used as a base reference. The variations of the average heat transfer coefficient, $\bar{h}$ and the average Nusselt number, $\overline{Nu}$ with Rayleigh number, Ra for the solid pin fin heat sink facing upward and sideward orientations are shown in Fig. 3. It can be observed that, at high Ra, $\bar{h}$ for sideward facing orientation is slightly higher than those for upward facing orientation. However, at low Ra, results showed an opposite trend (Fig. 3a), and subsequently the same behavior for the average $\overline{Nu}$ with Ra as can be noticed in Fig.3b. This results show that both orientations are of competitive nature depending on the fin structure and Rayleigh number as concluded by Huang et al. [12], and based on the data reported by Sparrow and Vemuri [7] who performed experimental investigation on round pin fin arrays and concluded that the upward facing orientation gave the highest heat transfer rates, followed by sideward facing and thereafter, downward facing ones. The phenomenon can be associated with induced plumes. For low fin population as in the present investigation, the heat transfer coefficients for sideward facing orientation are expected to be higher than those of upward arrangement. However for higher fin population, it is expected that the fins block some air flow and acts as a flow barrier for the sideward arrangement.

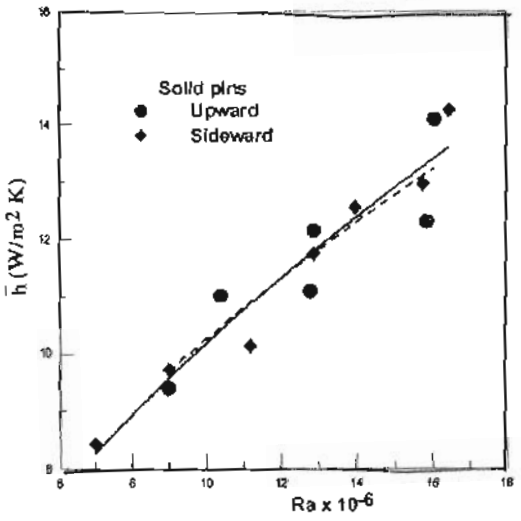

Fig.3a Average heat transfer coefficient versus Rayleigh number of solid pin fin heat sink for two different orientations

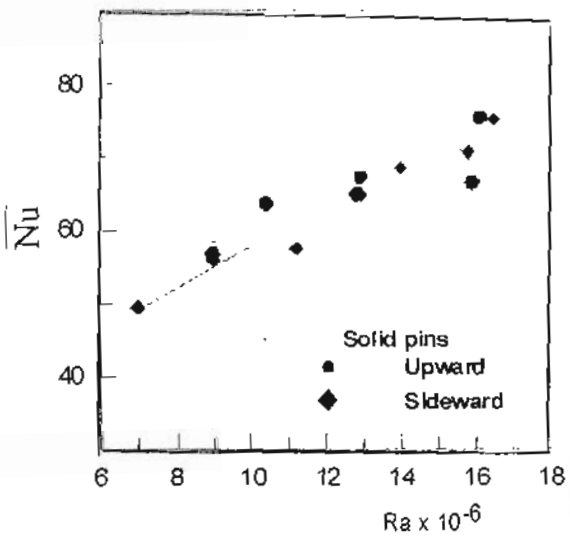

Fig.3b Average Nusselt number versus Rayleigh number of solid pin fin heat sink for two different orientations

4.2 Hollow/perforated pin fin heat sink

The experiments were carried out for three modules of vertical/horizontal base plate heat sink with different hollow pin inside-outside diameter ratio *(D_i/D_o=0.33, 0.5, 0.66)*. All modules had a staggered arrangement and of the same base plate dimensions, the same number of pin fins of fixed height. The variation of the average Nusselt numbers, $\overline{Nu}$ with Rayleigh number, Ra are investigated for both upward and sideward facing orientations over a Rayleigh number range of $4.5\times10^6 < Ra < 1.65\times10^7$.

Figure 4 indicates the variations $\overline{Nu}$ with Ra for the heat sink of hollow pin fins of D_i/D_o equals to 0.33 in both upward and sideward facing orientations. Values of $\overline{Nu}$ for sideward facing orientation are higher than those for upward orientation and the gap between them decreases with increasing Rayleigh number. $\overline{Nu}$ for sideward facing orientation exceeds by nearly 17% compared to that for upward facing orientation at mid tested range of Rayleigh number. This may be attributed to the increase of the induced plumes associated with the sideward arrangement in comparison with that associated with the upward arrangement.

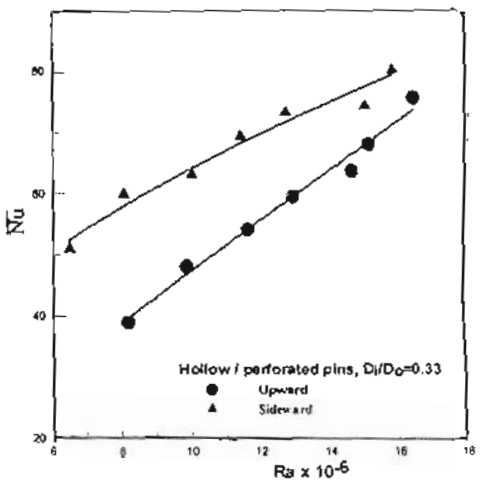

Fig. 4 $\overline{Nu}$ versus Ra of hollow/perforated pin fin heat sink for two different orientations, (D_i/D_o = 0.33)

The same behavior is observed for the hollow pin fin of D_i/D_o equals to *0.5* and *0.66* as shown in Fig. 5 and Fig. 6, respectively, where the average $\overline{Nu}$ for sideward facing orientations are also higher than those for upward facing orientation. The percentage increase in $\overline{Nu}$ for sideward facing orientation compared to that for upward facing orientation however, is reduced with increasing Di/D_o. This may be attributed to the presence of large diameter air column in the hollow/pins of low convective heat transfer coefficient with respect to that outside the pins, and the dependence of calculated average heat transfer coefficient on the total heat sink surface area, which increases with increasing D_i/D_o. This might diminished the improvement in heat transfer coefficient due to the effect of increasing intensity of induced plumes accompanied with larger D_i/D_o ratio.

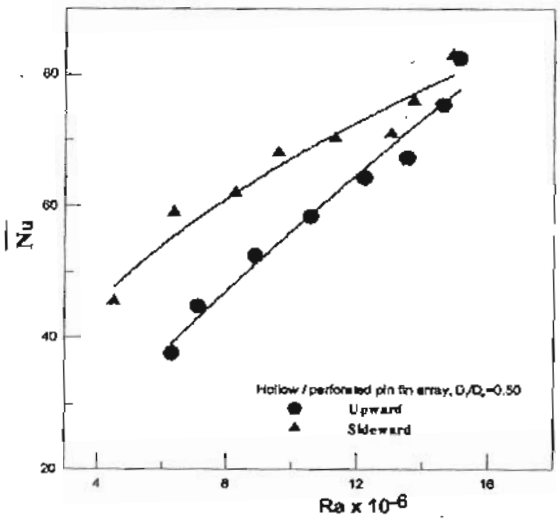

Fig. 5 $\overline{Nu}$ versus *Ra* of hollow/perforated pin fin heat sink for two different orientations, (Di/Do = 0.50)

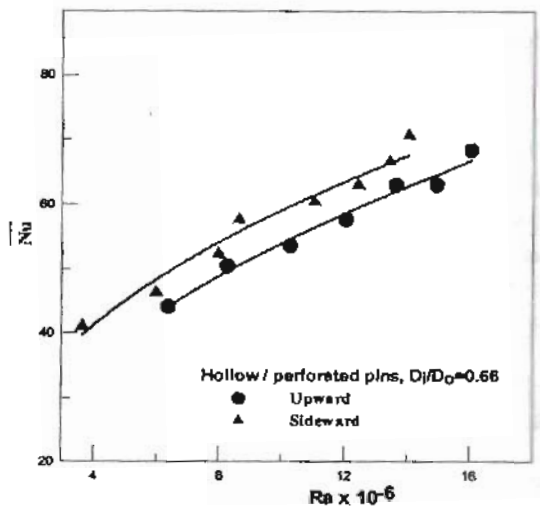

Fig. 6 $\overline{Nu}$ versus *Ra* of hollow/perforated pin fin heat sink for two different orientations, (D_i/D_o = 0.66)

A comparison of the values of $\overline{Nu}$ versus Ra for all tested heat sink modules in both upward and sideward facing orientation is shown in Figs. 7a and 7b, respectively. It can be observed that $\overline{Nu}$ for solid pin fin heat sink (lowest A_f/A_{bp}) over the tested range of Rayleigh number is the highest in both orientations. This is attributed to the increase of heat sink surface area, and hence the ratio of (A_f/A_{bp}) with hollow pin fins on which the average heat transfer coefficient is calculated. This is in agreement with the results of Huang et al. [12] who reported that the heat transfer coefficient increases with decreasing the finning factor, Ψ ($\Psi = A_f/A_{bp}$). The effect of the value of D_i/D_o on $\overline{Nu}$ for upward facing orientation (Fig. 7a) however, is different. The pin fins of larger D_i/D_o offered higher values of $\overline{Nu}$ at low Ra and had an opposite effect at higher values of Ra. This may be attributed to the increasing intensity of induced plumes with larger D_i/D_o, which might compensate the reduction in the calculated average heat transfer coefficient due to the increased heat transfer area.

The thermal performance of heat sink is measured by detecting the variation of the temperature difference between its base plate and surrounding air, ΔT with the heat input rate, Q_{in}. Figures 8a and 8b indicate the variation of ΔT with Q_{in} for all tested modules in both upward and sideward arrangements, respectively. Generally, the results indicate that ΔT increases with increasing heat input rate, Q_{in}. In addition, the temperature difference, ΔT decreases with increasing the hollow pin fin diameter ratio, D_i/D_o. The performance of sideward arrangement is also seen to be slightly higher than that of upward arrangement over the tested range of Rayleigh number. As reported in [12], the pin fin performance is also related to the heat sink porosity, ϕ which is defined as the volume fraction of air inside the heat sink (V_a/V_s); increasing the heat sink porosity is advantageous to both upward and sideward arrangements since it promotes the penetration depth of the ventilation.

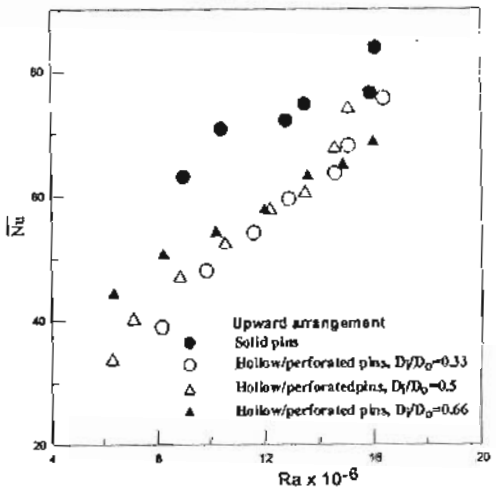

Fig. 7a Comparison of $\overline{Nu}$ variations with Ra of all tested pin fin heat sinks for upward facing orientation

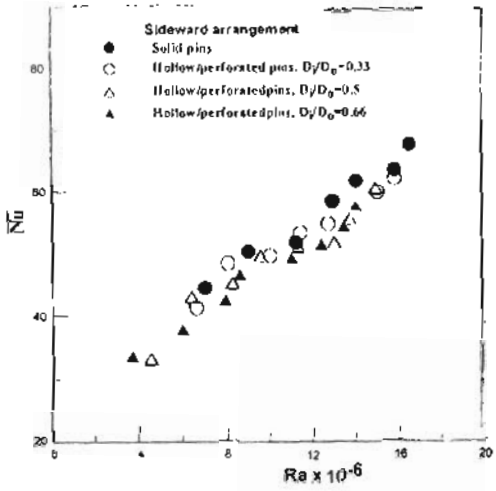

Fig. 7b Comparison of $\overline{Nu}$ variations with Ra of all tested pin fin heat sinks for sideward facing orientation

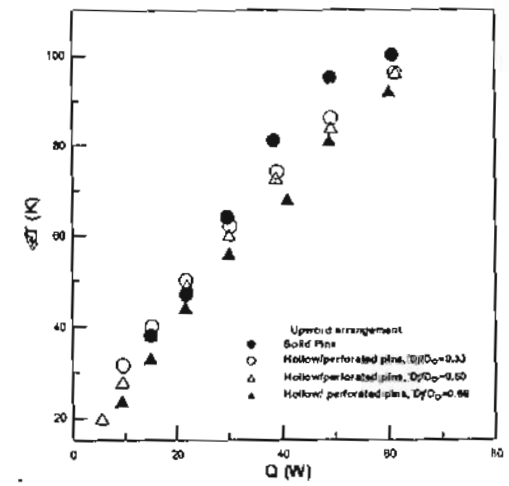

Fig. 8a Temperature difference, ΔT variations with heat input rate, Q_{in} of all tested pin fin heat sinks for upward facing orientation

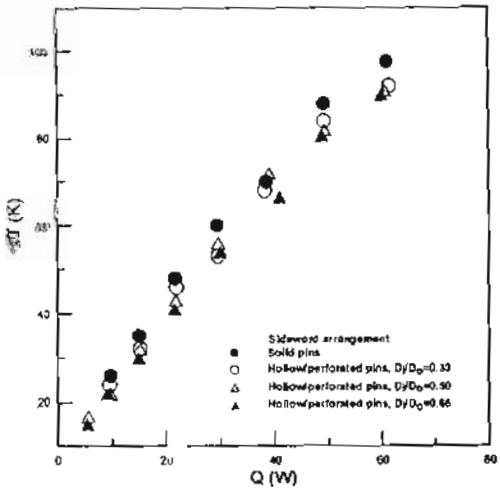

Fig. 8b Temperature difference, ΔT variations with heat input rate, Q_{in} of all tested pin fin heat sinks for sideward facing orientation

The test results of the present solid pin fin heat sink (A_f/A_{bp}=1.71, and ϕ = 0.95) in both upward and sideward facing orientations are compared with the data reported by Huang et al. [12] for one of the tested solid pin fin heat sink samples considered by them (Ψ= 1.758, and ϕ = 0.952). As can be noticed in Figs. 9, the average heat transfer coefficients of the present investigation are higher than those reported in [12], but have the same trend as theirs. These discrepancies may be attributed to the differences in fin structures and its population

for both the present heat sinks and those investigated by Hyang et al. [12].

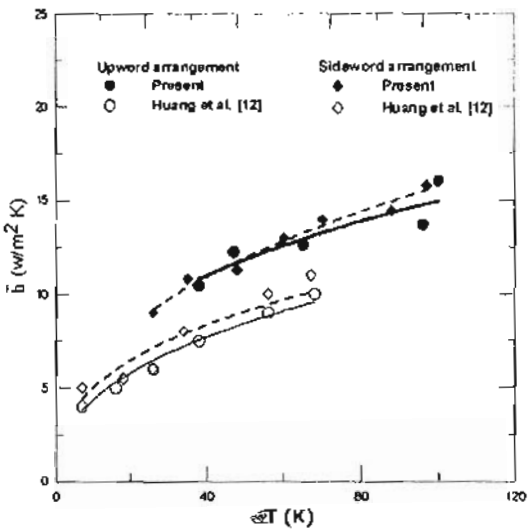

Fig. 9 Comparison of present results with the data given by Huang et al. [12] for solid pin fin heat sink of upward/sideward facing orientations

5. Conclusions

In the present study, the heat transfer characteristics of round hollow/perforated pin fin heat sinks subject to the influence of its geometry, heat flux and orientation are investigated under natural convection. Based on the preceding discussions, the following conclusions may be drawn:

1. Solid pin fin heat sink performance for upward and sideward orientations shows a competitive nature, $\overline{Nu}$ for sideward arrangement was slightly higher than those for upward arrangement at high Ra. However, at low *Ra*, the results showed an opposite trend.
2. For Hollow/perforated pin fin heat sinks, $\overline{Nu}$ of sideward arrangement was higher than those of upward arrangement, and the % increase of its value reduced with increasing the hollow pin diameter ratio, *Di/Do*.
3. Generally, the Solid pin fin heat sink yielded the highest $\overline{Nu}$ of both upward and sideward facing orientations. The average heat transfer coefficient was calculated based on the total heat sink surface area, which increases with the increasing D_i/D_o (50% saving in area with $D_i/D_o = 0.66$).
4. The temperature difference between the base plate and surrounding air, ΔT at the same heat input rate, Q_{in} was found less for hollow/perforated pin fin heat sink than that for solid pin one and its value decreases with increasing D_i/D_o. The performance of sideward arrangement is also seen to be slightly better than that of upward arrangement.
5. The present study appears to provide the first reported systematic study of the thermal performance of hollow perforated pin fin heat sink relying on natural convection.

References

1. Peng Y. Heat transfer and friction Loss Characteristics of pin fin cooling configurations, *J. Eng. Gas Turbines and Power* 1984; 106: 246-251.
2. Brigham B. A. and VanFossen G. J. Length to diameter ratio and row number effects in short pin fin heat transfer, *J. Eng. For Gas Turbines and Power* 1984; 106: 241-245.
3. Tanda G., Heat Transfer and pressure drop in a rectangular channel with diamond shaped elements, *Int. J Heat Mass Transfer*, 2001; 44: 3529-3541.
4. Armstrong J. and Winstanely D., A review of staggered array pin fin heat transfer for turbine cooling applications, J. Turbo machinery 1988; 110: 94-103.

5. Kraus A.D., Aziz M. and Welty J. Extended surface Heat Transfer, New-York: Wiley, 2002: 190-206.
6. Kraus A. D. and Bar-Cohen A. Design and Analysis of Heat sinks, New-York: Wiley 1995: 286-320.
7. Sparrow E. and Vemuri S., Natural convection/radiation heat transfer from highly populated pin-fin arrays, *Int. J. Heat Mass Transfer*, 1985; 107: 190-197.
8. Sparrow E. and Vemuri S., Orientation effect on natural convection/radiation heat transfer from pin-fin arrays, Int. J. Heat Mass Transfer 1986; vol. 29,no. 3: 359-368.
9. Alessio M. E. and Kaminski D. A., Natural convection and radiation heat transfer from an array of inclined pin fins, ASME, Transactions, Journal of Heat Transfer 1989;
10. 111: 197-199.
11. Zografos A.I. and Sunderland J.E., Natural convection from pin fin arrays, Exper. Therm. Fluid Sci. (1990); 3: 440-449.
12. Aihara T., Maruyama S., and Kobayakawa S., Free convection/ radiative heat transfer from pin-fin array with a vertical base plate (general presentation of heat transfer performance), *Int. J. Heat Mass Transfer* 1990; 33, no. 6: 1223-1232.
13. Huang R.T., Sheu W.J., and Wang C.C. Orientation effect on natural convective performance of square pin fin heat sinks, *Int. J. Heat Mass Transfer*, received in revised form in 14 August, 2007.
14. Enchao Y. and Yogendra J., Heat transfer enhancement from enclosed discrete components using pin-fin heat sinks 2002; 45: 4957-4966.
15. Sahray D., Magril R., Dubovsky V., Gennady Z., and Letan R., Natural convection heat transfer from pin fin heat sinks with horizontal base, 13th International Heat Transfer Conference (2006).
16. Bahadur R. and Cohen A.B., Thermal Design and Optimization of Natural Convection Polymer Pin Fin Heat Sinks, IEEE Transactions on Components and Packaging Technologies 2005; pp. 1-9.
17. Peterson G. P. and Ortega A., Thermal control of electronic equipment and devices, *Adv. Heat Transfer* 1990; 20: 134-181.
18. Fisher T.S. and Torrance K.E., Free convection limits for pin fin cooling, J. Heat Transfer 1998; 120 (3): 633-640.
19. Kobus C.J. and Oshio T., Development of a theoretical model for predicting the thermal performance characteristics of a vertical pin fin array heat sink under combined forced and natural convection with impinging flow, *Int. J. Heat Mass Transfer* 2005; 48 (6): 1053-1063.
20. Kobus C.J. and Oshio T., Predicting the thermal performance characteristics of staggered vertical fin array heat sinks under combined mode radiation and mixed convection with impinging flow. *Int. J. Heat Mass Transfer* 2005; 48 (13): 2684-2696.
21. Kline S.J. and McClintock F.A., Describing uncertainties in single sample experiment. Mech. Eng. 1953, 75: 3-8.